scientific reports

Check for updates

OPEN

Use of micro-computed tomography to monitor olive fruit damage caused by three insect pests

Javier Alba-Tercedor ✉ & Francisca Ruano ✉

A complete three-dimensional reconstruction of the internal damage (oviposition holes, entry and exit galleries, cavities caused by fungal infection) of three destructive pests of olive fruit was obtained using micro-computed tomography. In the case of the olive fruit fly (*Bactrocera oleae*), complete reconstruction of the galleries was achieved. The galleries were colour-coded according to the size of the internal lumens produced by larval instars. In the case of the olive moth (*Prays oleae*), we confirmed that the larvae only consume olive stones, leaving pulp tissue intact. This study revealed the evolutionary defensive adaptation developed by larvae, creating entrance/exit gallery in the form of a zigzag with alternating angles to avoid the action of possible parasitoids. In the case of olive fruit rot, caused by fungal infection transmitted by the midge (*Lasioptera berlesiana*), microtomography revealed the infection cavity, which was delimited by a protective layer of tissue produced by the plant to isolate the infection zone, which contained fungal hyphae and reproductive organs of the fungus. Two ovoid cavities were observed below a single external orifice in the concave necrotic depression. These results were interpreted as successive ovipositions of *B. oleae*, followed by the parasitoid *L. berlesiana*. High-resolution 3D rendered images are included as well as supplementary videos that could be useful tools for future research and teaching aids.

Olive trees are grown all over the world, with high yields found in regions with Mediterranean climates. Olive oil is currently produced in more than 40 countries, with more than 750 million olive trees cultivated worldwide, 95% of which are in the Mediterranean region[1]. It remains the most widely cultivated perennial crop in the region, and it is well suited to its climate, which is characterised by high temperatures and hydric stress[2].

Globally, on average, 10–28% of crop production is lost to pests[3,4]. In the case of olive crops, alarming statistics show that up to 40% of global olive production is lost annually because of their impact[2]. Several insects, pathogens, and nematodes affect olive trees and threaten olive production; however, olive cultivation is considered a stable crop. In this cultivation, some exclusive insect pests are associated with different incidences in olive fruit, affecting the yield and/or quality of olive oil and olive table. In order of economic importance[2], the pests studied are as follows:

1. The "olive fruit fly" *Bactrocera oleae* (Gmelin, 1790) (Diptera: Tephritidae). It is considered the most important olive pest in the Mediterranean region and has been recorded in 34 countries in the Mediterranean and the Middle East, as well as in southern and eastern Africa, India, and Pakistan, and has been detected in California and Mexico since the end of the twentieth century[2]. This insect has several generations per year (usually 2–4, but up to 6 depending on the prevailing temperature and availability of fruit). The female can lay up to 20 eggs/day on the fruit, producing several hundred eggs during her lifetime. The oviposition damage the fruit. Larvae feeding inside the fruit mesocarp, damaging the fruit and reducing its quality for commercial sale. It can also cause premature ripening or splitting of the fruit, loss of oil quality, or complete loss of damaged fruit in table olives. Infestation can be severe enough to cause a 100% fruit drop in years of low yield[5]. Some authors have noted that some fungi share at least part of their life cycle with the olive fruit fly because they mainly affect fruits from the beginning of olive ripening and could be favoured by insects that can act as vectors[6].

Department of Zoology, Faculty of Sciences, University of Granada, 18071 Granada, Spain. ✉email: jalba@ugr.es; fruano@ugr.es

2. The "olive moth" *Prays oleae* (Bernard, 1788) (Lepidoptera: Plutellidae, Prayninae)[7]. *P. oleae* is widespread throughout the Mediterranean and is considered the second most important olive pest in the EU. *P. oleae* completes three generations on the olive tree each year, damaging the flowers, leaves, and fruits in each generation. In carpophagous generation, which is the most dangerous for yield, eggs are laid on the calyx of young olive fruit; the larvae enter the young fruit endocarp near the pedicel during the summer and feed on the olive seeds, dehydrating the fruit and causing it to drop, especially when the larvae leave the olive fruit to pupate in the soil. This has a negative impact on the olive harvest[2]. A 28-year study by Ramos et al.[8] in southern Spain (Andalusia) showed that this pest can reduce olive production by 50–60%, with heavy infestations occurring approximately every 3 years, causing 40% premature fruit drop and consequently significant economic losses.
3. The "olive fruit rot" appears because of a fungal infection, which can be caused by different species of fungi. The most common species is *Botryosphaeria dothidea* (Moug.) Ces. & De Not[9,10]. Revisions of the names of the fungi involved in olive fruit rot and taxonomic changes are presented in Lazzizera et al.[9]. This pathogen is the causative agent of the Dalmatian disease of olives, which occurs in most of the Mediterranean basin[10,11]. *B. dothidea* produces a sunken, necrotic, and circular lesion (approximately 8 mm in diameter, never larger than 1 cm) with a sharp edge that separates the infected tissue from the healthy fruit tissue; this appearance is called "escudete" (little shield) in Portuguese and Spanish. As the disease progresses, necrotic depression expands and covers the entire fruit. As the fruit ripens, it falls to the ground and becomes mummified[11]. Overall, the incidence of olive fruit with Dalmatian symptoms is relatively low, but it often exceeds the tolerance level for the "Extra" class standard for olive fruit, which is usually at a level of 2% or 4%, according to Spanish law[12] or the FAO's Codex Alimentarius[13]. Its presence on table olives is particularly important[14]. Thus, oviposition wounds may facilitate fungal infection. Iannotta et al.[10] observed a correlation between the presence of *Botryosphaeria* olive rots, which were formerly associated with the fungus *Camarosporium dalmaticum* (Dalmatian disease), and olive fly infestation, but did not provide evidence of the role of the insect in favouring fungal infections[6]. The larvae of midge *Lasioptera berlesiana* Paoli, 1907 (Diptera: Cecidomyiidae)[15] are active eggs consumers. Subsequently, the species has been used as a biological control agent for the olive fruit fly[16]. There is evidence of its role in transmitting fungi, but its interaction with the olive fruit fly and its transmission remains controversial[17–19].

To study the effects of these pests and diseases on olive fruits, ocular inspections followed by dissection of the fruits, accompanied or not by light microscopy or electron microscopy studies, have been carried out (i.e. Refs.[20,21]). Recently, X-ray images have been used to determine the degree of infection in fruit[22]. In this study, the technique of computerised microtomography is used for the first time to study the fruit as a whole and, without altering it, to obtain high-resolution 3D rendered images of the effects of the three pests. Studying each component in its original situation, allowing observations from different perspectives, obtaining high-quality 3D rendered images, and obtaining additional supplementary videos as useful tools for future research and teaching aids.

Materials and methods

Olive fruits

In accordance with relevant institutional, national, and international legislation and guidelines, olives were harvested in 2023, in late summer, close to autumn, in olive groves in the mountains near the city of Granada in southern Spain. Olives with external signs of attack were transported to the laboratory. These were X-rayed in the microtomograph, and one of each type of pest was selected for scanning and reconstruction to obtain rendered images of figures and supplementary videos.

Micro-CT scans

For microtomographic study, fresh olive fruits with signs of attack were mounted on top of a polypropylene tube and were fixed to the sample holder with plasticine (Figs. 4a, 5a). A SkyScan 1172 desktop high-resolution microtomograph, upgraded to a Hamamatsu L702 (100/250) source and a Ximea 11Mp camera, was used. The scanning parameters were set up as follows: 0.5 mm aluminium filter, voxel size = 13.54 µm^3, 48 kV, 124 µA, 2 × 2 camera binning, 180º rotation and a rotation step = 0.47°. For a detailed study of the concave necrosis of olive fruit rot (Fig. 5d,f–i), the scanning parameters were changed as follows: voxel size = 0.94 µm^3, rotation step = 0.5°.

Image reconstruction

Bruker Micro-CT Skyscan (https://www.bruker.com/products/microtomography.html) *NRecon* software (v.2.0.0.5) was used to reconstruct the TIFF X-ray images, and CTAnalyser v.1.20.8.0 was used for the primary "cleaning" process. The resulting images were reoriented with *DataViewer* v.1.6.0.0), and *CTvox* v.3.3.1 was used to obtain the 3D rendered images of Fig. 1c–f and some scenes marked with the *CTvox´*s logo in Supplementary Video S1, as previously described[23]. FEI's *Amira* software (v. 2019.3)[24,25] was used to obtain 3D rendered images (Figs. 1b,f–h, 2, 3, 4c–f, 5b–i) and Supplementary Videos S1–S3. The built-in colour filter "volrenRed.col" was used to obtain the colour of Amira's rendered images (Fig. 5d,f–i) and Supplementary Video S1.

To isolate the galleries burrowed by olive fruit fly larvae and obtain a colour code according to their lumen diameter, a similar methodology was used as previously described to reconstruct the tracheal tubes of the coffee borer beetle[26]. Thus, colour-coded images were created using the 3D analysis plug-in in the *CTAnalyser*'s customised processing tab and saved to determine the structure thickness (or separation) as done previously[27] and as described in a Bruker microCT method note[28]. In the resulting new set of images, an arithmetic operation with CTAnalyser was performed by multiplying by 20 and uploading them to CTvox to obtain 3D rendered

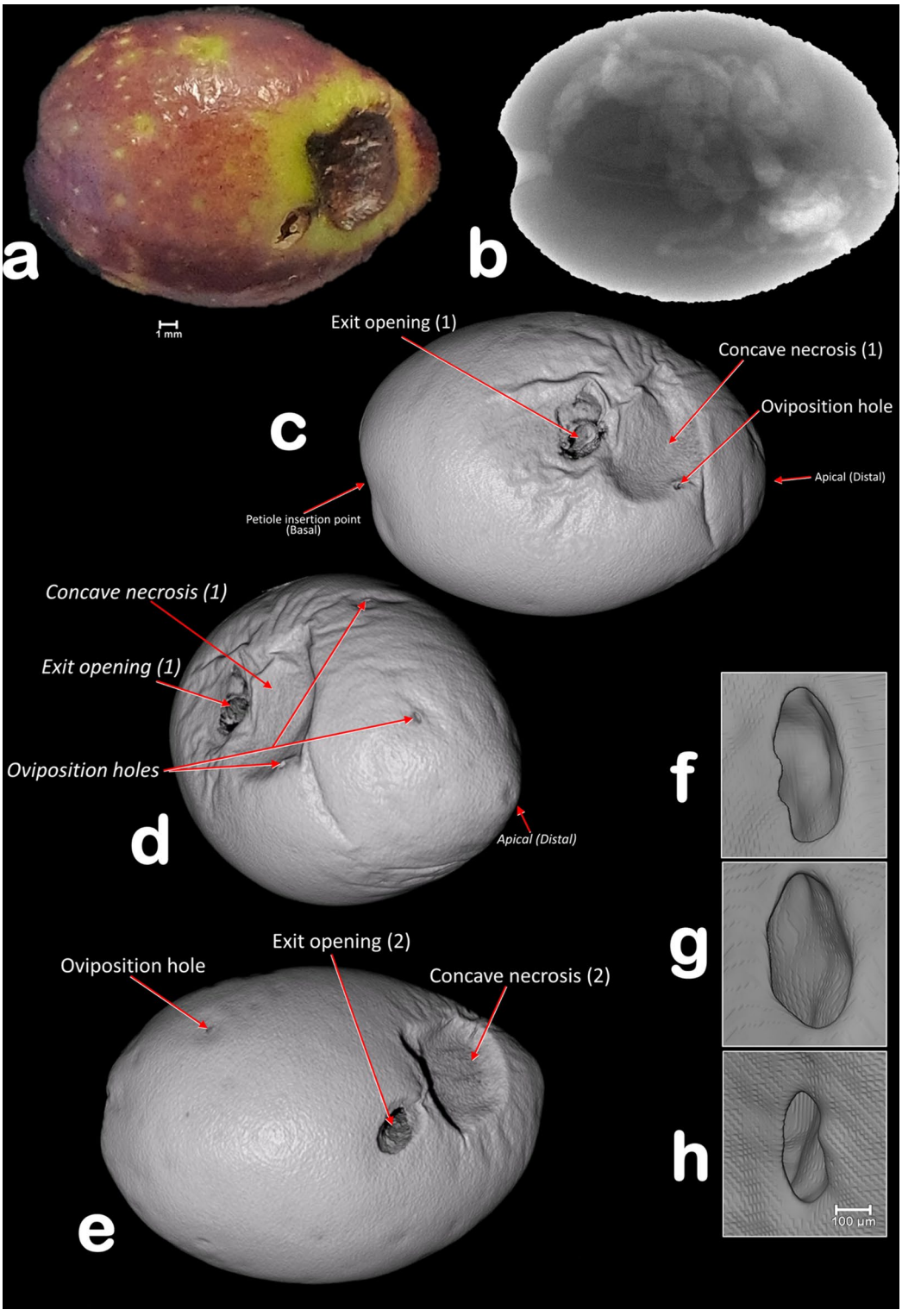

Fig. 1. Olive fruit attacked by the olive fly *Bactrocera oleae*. External damage observed on a fresh olive fruit (**a**), X-ray projection image (**b**), and micro-CT rendered images of its external surface (**c**–**e**). Oviposition holes (**f**–**h**).

images and record the videos of Supplementary Video S1 or uploaded to Amira, performing a registration with the entire olive fruit and changing the transfer colour curves to obtain the same colour code as the one obtained with *CTvox* to obtain images of Figs. 2 and 3 and Supplementary Video S1.

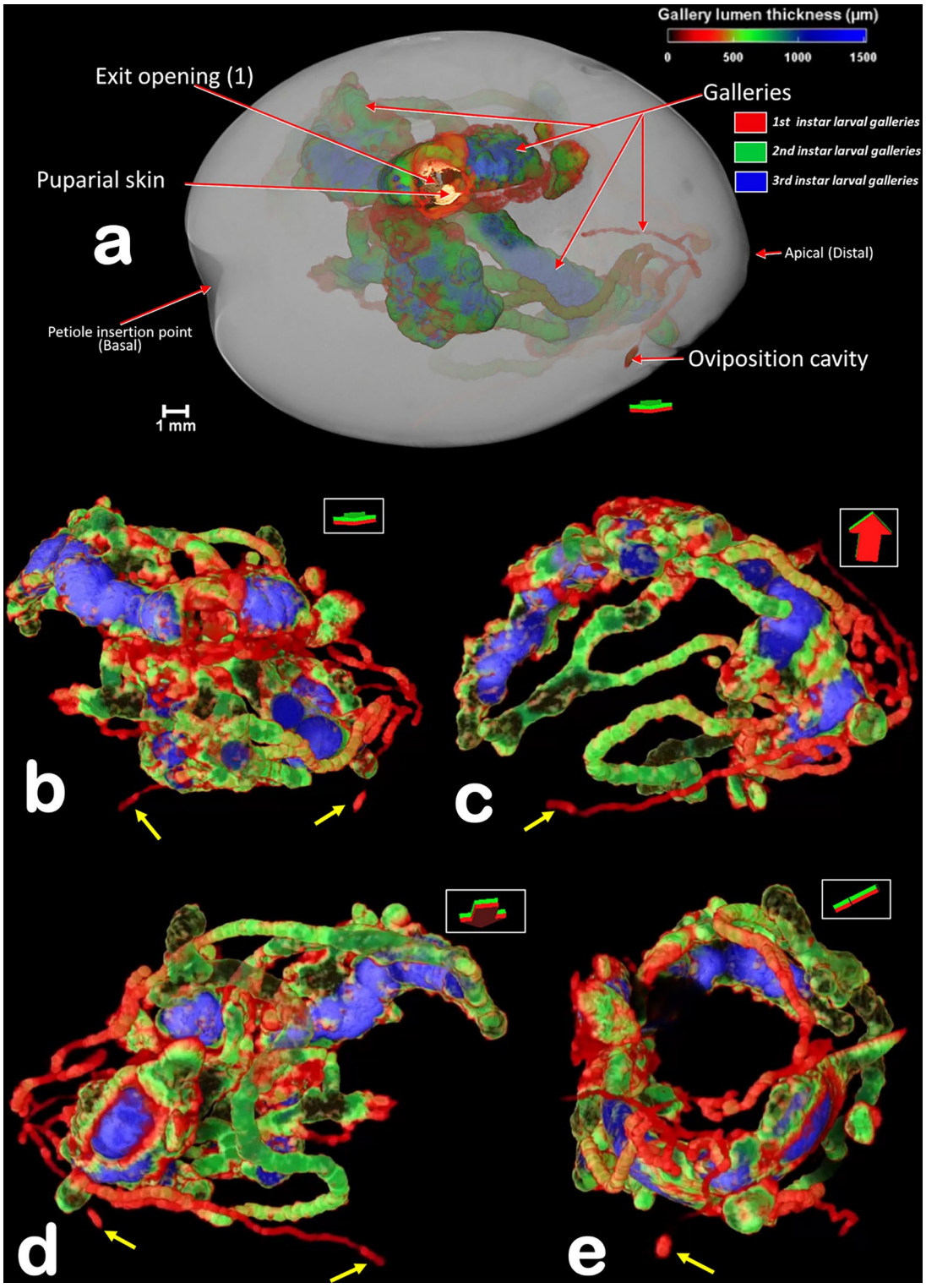

Fig. 2. Micro-CT rendered images of internal galleries excavated by larvae of the olive fruit fly *Bactrocera oleae*. The olive fruit is made transparent (**a**), and only the galleries have been isolated so that they can be viewed from different perspectives (**b**–**e**). Yellow arrows indicate oviposition cavities. The lumen diameter is in accordance with the colour scale of the bar shown on the upper right. Three areas of lumen galleries were observed, corresponding to the three larval instars (shown in red, green and blue, respectively, corresponding to instars L1–L3).

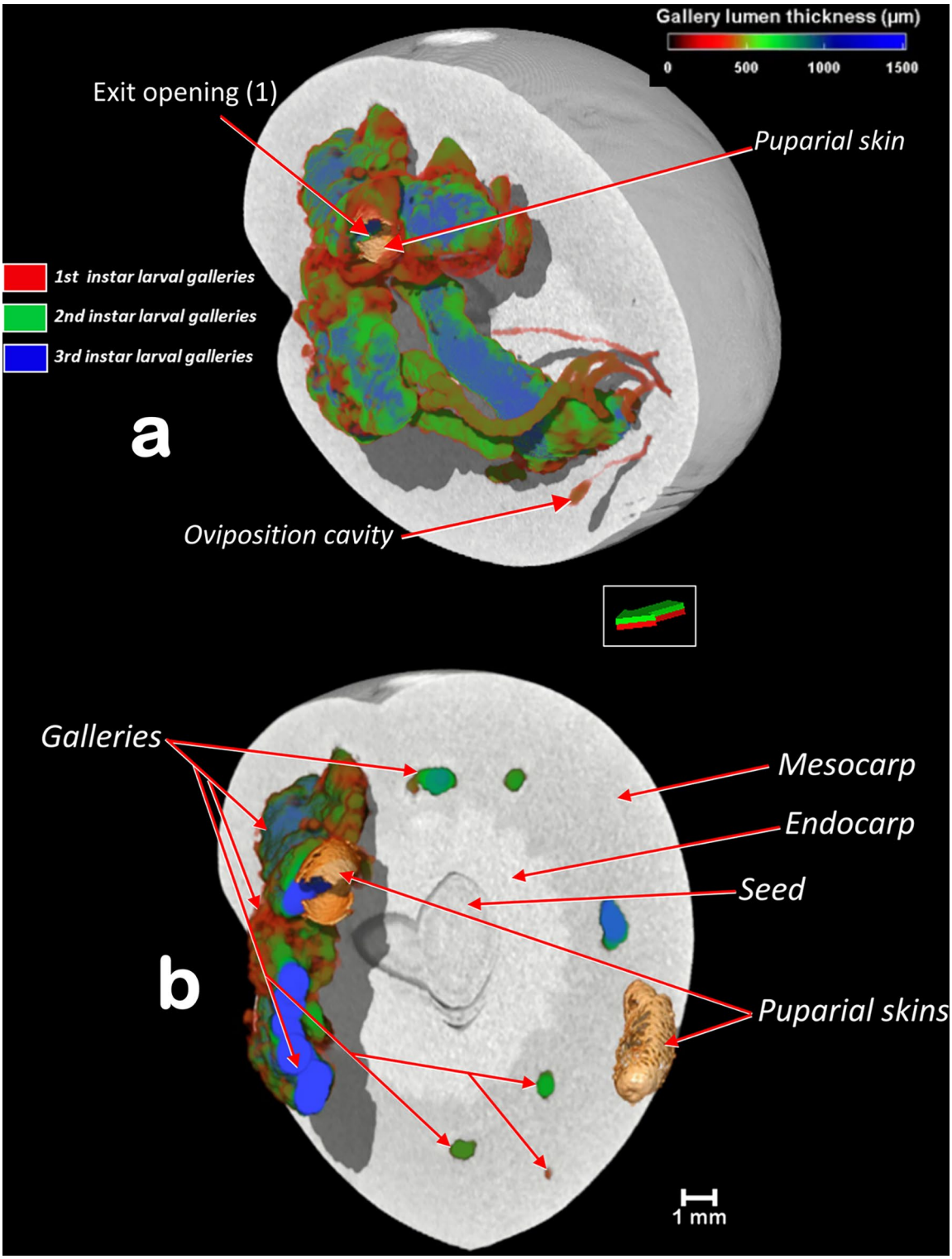

Fig. 3. Micro-CT rendered images of the internal galleries excavated by the larvae of the olive fruit fly *Bactrocera oleae* in sagittal (**a**) and transverse sections (**b**). The lumen diameter is in accordance with the colour scale of the bar shown on the upper right. Three areas of luminal galleries were observed, corresponding to the three larval instars (shown in red, green and blue, respectively, corresponding to instars L1–L3).

Macrophotographs

The olive fruit macrophotographs in Figs. 1a, 4a, and 5a and Supplementary Videos S1–S3 were taken using a Samsung Galaxy Note10+ smartphone.

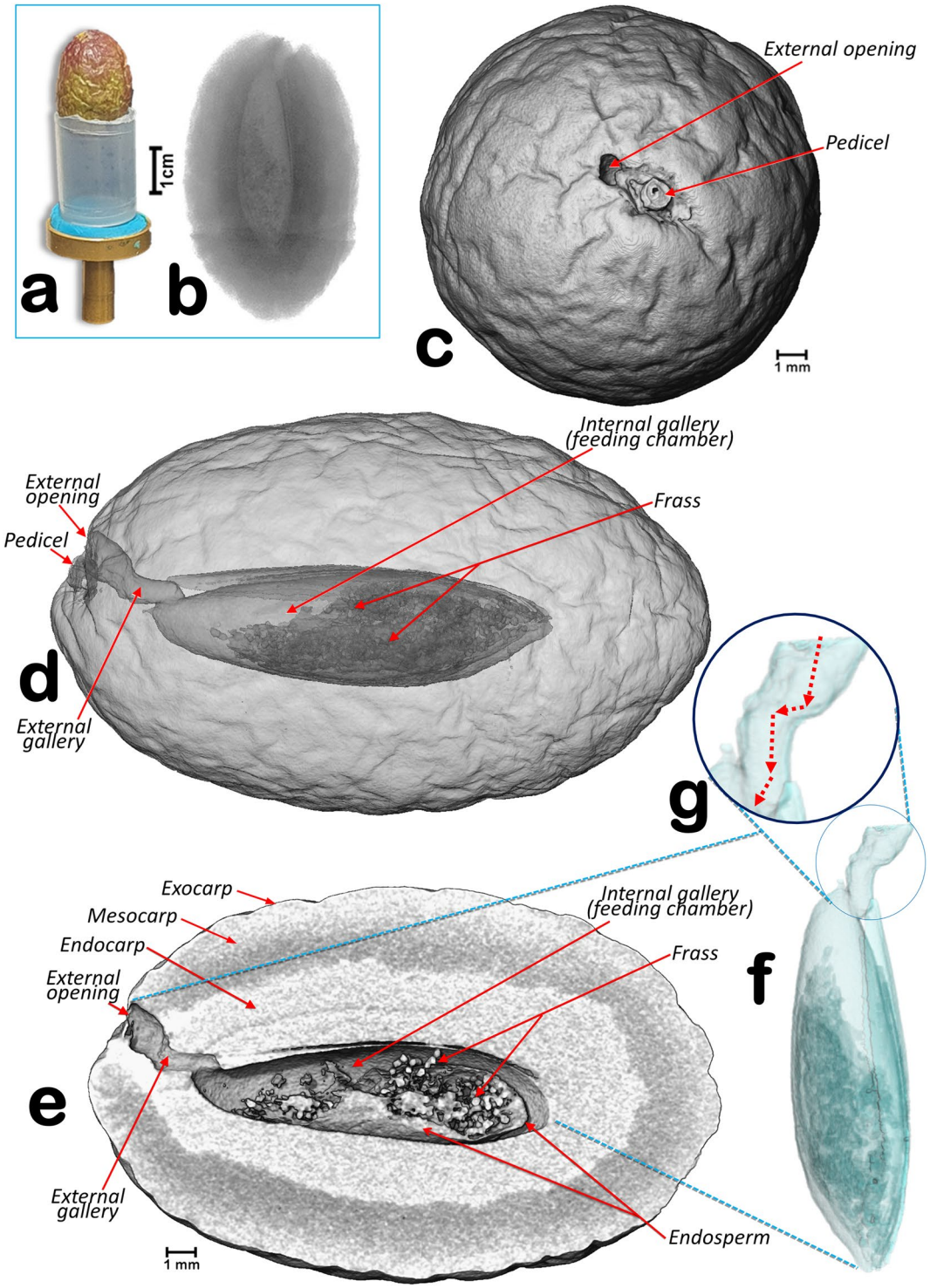

Fig. 4. Olive fruit attacked by the olive moth *Prays oleae*. Olive fruit mounted in a sample holder for scanning (**a**). X-ray projection image (**b**). Micro-CT rendered images (**a**–**f**). Transparent surface view of the internal cavities (**d**). Sagittal section (**e**). Reconstruction of the cavities excavated by the moth (**f**, **g**). The dotted red arrows (**g**) are helpful for visualising the alternating angles in the gallery following the external (entry/exit) opening.

Results

Microtomography revealed the different parts of the fruit, both on the external surface (exocarp) and internally

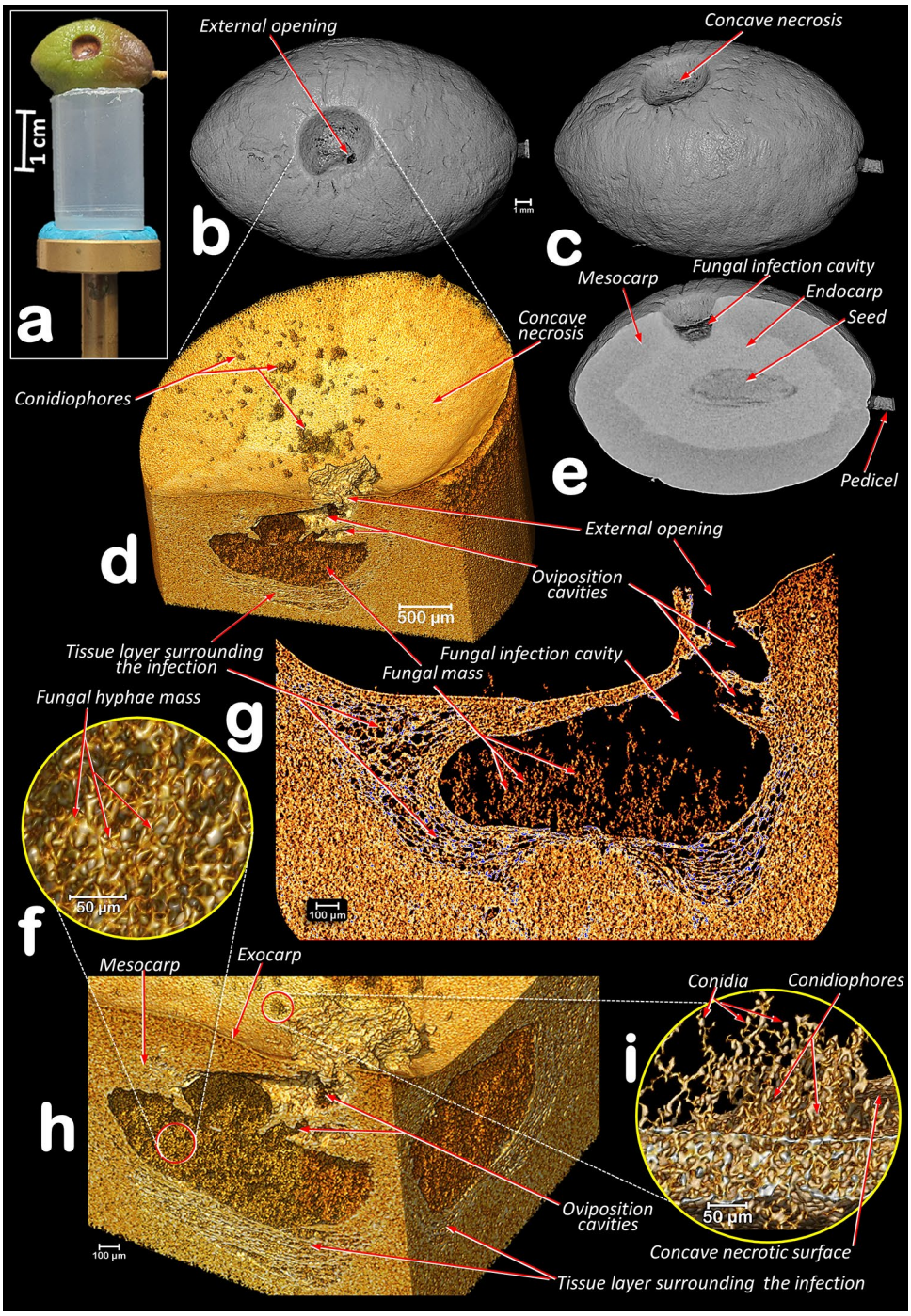

Fig. 5. Olive fruit affected by fruit rot (shield) fungal disease. The olive fruit is mounted in a sample holder for scanning (**a**). Micro-CT rendered images (**b**–**i**). External views (**b**, **c**). Sagittal-section view (**e**). Virtual core extraction at the concave necrosis level (**d**, **h**). Multiplanar 13 µm slice (**g**). High-magnification images of the fungal mass in the cavity (**f**) and the fungal reproductive structures on the surface of the concave necrosis (**i**).

in the pulp (mesocarp and endocarp), the endosperm surrounding the seed, and the effects of the activity of three highly damaging pest diseases that are widely distributed throughout the Mediterranean region (Figs. 1, 2, 3, 4, 5 and Supplementary Videos S1–S3).

The "olive fruit fly" *Bactrocera* oleae (Figs. 1, 2, 3, and Supplementary Video S1)

The olive fruit studied (Fig. 1, and Supplementary Video S1) exhibited several oviposition holes. These have a common roughly elliptical shape (Fig. 1f,g), with a minor axis of 202.9 ± 36.6 µm and a major axis of 416.8 ± 52.3 µm (n = 4 wounds, mean ± SD). In general, an oviposition cavity followed by a narrower gallery that

widens can be observed (Fig. 2a–d). Some oviposition holes did not extend into the galleries (Fig. 2e). In the reconstructed 3D rendered images of the galleries with a colour code according to lumen thickness (Fig. 2a–e), we obtained three different colour groups(red, green and blue), corresponding to the three larval instars (L1–L3). An increasing thickness of the gallery lumen occurs during larval development, with a diameter of up to 500 µm for the galleries of the first instar larvae (red), 500–800 µm for the galleries of the second instar larvae (green) and approximately 800–1500 µm for the galleries of the third instar larvae (blue). We did not detect fungal growth, and the external concave necrotic cavity associated with the pupal chamber did not appear directly related to the feeding galleries. In the widest part of the galleries and close to the exit hole, we found two pupal skins (Fig. 3a,b).

The "olive moth" *Prays oleae* (Fig. 4, and Supplementary Video S2)

The studied olive fruit presented a single external opening near the pedicel (Fig. 4c–f). From this external orifice, a short gallery with an alternating angle forms a zig-zag path that starts (Fig. 4d–g) communicating with a large central feeding chamber. This resulted from the consumption of olive stone (both cotyledons are consumed), and frass deposits are observed (Fig. 4d–f). The mesocarp and endocarp are not affected.

The "olive fruit rot" (Fig. 5 and Supplementary Video S3)

The olive fruit studied exhibits a typical olive shield rot syndrome, which is externally visible through a concave necrosis area (ca. 5 mm wide) on the fruit surface (Fig. 5a–e). Micro-CT images revealed the fungal infection, along with the reproductive structures (conidiophores and conidia). We found these structures on the surface of the concave necrosis (Fig. 5d,h,i) and inside, the fungal infection cavity, filled with a fungal mass of hyphae (Fig. 5f–i). Infection causes the proliferation of cells that form a layer that surrounds and encapsulates the infection cavity (Fig. 5d,g,h). One single external opening can be observed (Fig. 5a,d,g,h). Nevertheless, we located in the vicinity of this hole, two oviposition cavities, one more external and larger than the other but contiguous and both below the larger cavity (Fig. 5d,g,h). No insect remains or pupal skin appears.

Discussion

Although it has previously been pointed out that the olive fruit fly produces a single puncture per olive[18], it is known that this may be more when there is a small yield with a low number of olive fruits available[1,29]. In the studied olive fruit, we detected five ovipositional punctures, from which only three continued with galleries and two reached the adult stage (two pupal skins). In recent years, there has been a significant decrease in crop yields in some areas due to drought caused by climate change, justifying the high infestation rate.

Some oviposition punctures or wounds do not correspond to laid eggs, as females with immature ovaries also try to lay eggs[30]. In any case, many authors refer to them as alive and non-alive or false punctures during olive fly oviposition[31], either because the eggs have not developed or there has been a puncture without an egg being laid because the ovarioles are not fully developed. In our studied olive fruit infested by *B. oleae*, some punctures had to be sterile because no gallery developed at all. Gonçalves et al.[32] reported a mortality in laid eggs of 2.6–16.6%. Some of these damaged eggs were possibly provoked by *L. berlesiana*. However, in our study, olive fruit affected by *L. berlesiana* did not have any remnants of *B. oleae* galleries, frass, or exuviae. The destruction of the olive fly egg should occur almost immediately after oviposition. With respect to *B. oleae* damage in olive fruit, we found an external concave necrosis depression that was not directly linked to the pupal chamber or feeding galleries. This finding agrees with the possibility that this depression was caused by a high accumulation of secondary metabolites surrounding the pupal galleries, but not by fungal proliferation, as previously suggested[21].

With respect to olive fruit attacked by the olive moth *P. oleae*, we found a single short external gallery, which was detected in other insects that consume the internal parts of fruits and seeds[33]. This single gallery exhibits alternating angles forming a zig-zag tunnel, as previously reported for the coffee berry borer beetle[34]. This strategy may hinder the access of some parasitoids to the larva of the first or last instar when situated near the fruit surface and is adaptative for this type of fruit mining insects. We also obtained evidence that the larvae of *P. oleae* used the same gallery to enter and exit the olive seed but enlarged the exit gallery and triggered the drop of olive fruit, because no signal from another tiny entry gallery appeared at all. In any case, the larva remained exclusively in the olive stone, revealing that pulp (either the mesocarp or the endocarp) was unaffected and that the entire inner part of the olive stone was consumed (both cotyledons). The feeding cavity resulted partially occupied by frass.

In the olive fruit rot study, we deduced that the two oviposition cavities observed in the vicinity of the external opening correspond to *B. oleae* (the larger) and the smaller one to *L. berlesiana*. Thus, a single external opening should correspond to the exit hole of *L. berlesiana* larvae, which immediately after they leave the olive fruit pupate in the soil[35].

Conclusions

The use of micro-CT to study the damage caused to olives by three different pests has allowed us to complete a three-dimensional reconstruction of the internal damage they provoke (oviposition marks/holes, entrance/exit galleries, cavities caused by fungal infection). In the case of the olive fruit fly (*B. oleae*), we performed a complete reconstruction of the galleries and their separation into colour codes according to larval instar size. Even in the galleries corresponding to L1, their narrow lumen shows a "rosary" shape because of successive bites, as small larvae consume pulp and advance by digging in a tunnel. It was also possible to identify the oviposition sites that failed (either because they were the work of immature females or because the eggs were not fertile).

Regarding olive moths, we confirmed that they only consume olive stones. This study showed that the larva leaves the rest of the fruit intact, and we revealed the evolutionary defensive adaptation that the larva has developed by making the entrance gallery in the form of a zigzag, with alternating angles, to avoid the action of parasitoids.

In the case of olive fruit rot, microtomography revealed a cavity, filled with fungal hyphae, and its reproductive organs. In addition, two ovoid cavities, one larger than the other, were observed in the vicinity of the external orifice. We deduced that these were the successive ovipositions of *B. oleae* and its parasitoid *L. berlesiana*.

In addition to detailed high-resolution 3D rendered images, supplementary videos were included, which could be useful tools for future research and valuable teaching aids.

Data availability

The datasets generated and analysed during the study are available from J.A.-T. upon reasonable request, and always within the framework of a collaborative scientific project.

Received: 20 March 2024; Accepted: 3 September 2024
Published online: 09 September 2024

References

1. EIP-AGRI Focus Group. Pests and diseases of the olive tree. 1–32 (2020).
2. Lantero, E., Matallanas, B. & Callejas, C. Current status of the main olive pests: Useful integrated pest management strategies and genetic tools. *Appl. Sci.* **13**, 12078 (2023).
3. Savary, S. *et al.* The global burden of pathogens and pests on major food crops. *Nat. Ecol. Evol.* **3**, 430–439 (2019).
4. IPPC Secretariat. 2021. *Cientific Review of the Impact of Climate Change on Plant Pests—A Global Challenge to Prevent and Mitigate Plant Pest Risks in Agriculture, Forestry and Ecosystems. Rome. FAO on Behalf of the IPPC. Scientific review of the impact of climate change on plant pests—A global challenge to prevent and mitigate plant pest risks in agriculture, forestry and ecosystems. Rome. FAO on behalf of the IPPC Secretariat*. https://doi.org/10.4060/cb4769en (2021). https://doi.org/10.4060/cb4769es.
5. Petacchi, R. *et al. Pest Management in Olive Orchards. Botany and Production* (CAB International, 2023).
6. Malacrinò, A., Schena, L., Campolo, O., Laudani, F. & Palmeri, V. Molecular analysis of the fungal microbiome associated with the olive fruit fly *Bactrocera oleae*. *Fungal Ecol.* **18**, 67–74 (2015).
7. PESI portal—*Prays oleae* (Bernard, 1788). http://www.eu-nomen.eu/portal/taxon.php?GUID=urn:lsid:faunaeur.org:taxname:434186.
8. Ramos, P., Campos, M. & Ramos, J. M. Long-term study on the evaluation of yield and economic losses caused by *Prays oleae* Bern. in the olive crop of Granada (southern Spain). *Crop Protect.* **17**, 645–647 (1998).
9. Lazzizera, C., Frisullo, S., Alves, A. & Phillips, A. J. L. Morphology, phylogeny and pathogenicity of *Botryosphaeria* and *Neofusicoccum* species associated with drupe rot of olives in southern Italy. *Plant Pathol.* **57**, 948–956 (2008).
10. Iannotta, N., Noce, M. E., Ripa, V., Scalercio, S. & Vizzarri, V. Assessment of susceptibility of olive cultivars to the *Bactrocera oleae* (Gmelin, 1790) and *Camarosporium dalmaticum* (Thüm.) Zachos & Tzav.-Klon. attacks in Calabria (Southern Italy). *J. Environ. Sci. Health B* **42**, 789–793 (2007).
11. Moral, J., Muñoz-Díez, C., González, N., Trapero, A. & Michailides, T. J. Characterization and pathogenicity of Botryosphaeriaceae species collected from olive and other hosts in Spain and California. *Phytopathology* **100**, 1340–1351 (2010).
12. BOE-A-2001-21717 Real Decreto 1230/2001, de 8 de noviembre, por el que se aprueba la Reglamentación técnico-sanitaria para la elaboración, circulación y venta de las aceitunas de mesa. https://www.boe.es/buscar/doc.php?id=BOE-A-2001-21717.
13. Organización Mundial de la Salud & Organización de las Naciones Unidas para la Alimentación y la Agricultura. Norma Para los Aceites de Oliva y Aceites de Orujo de Oliva. *Codex Alimentarius* **1**, 1–9 (2017).
14. N. Gonzalez , E. Vargas Osuna, A. T. EL escudete, una enfermedad relevante en aceituna de verdeo. *Vida Rural* 56–58 (2006).
15. PESI portal - Search. https://www.eu-nomen.eu/portal/search.php?search=simp&txt_Search=Lasioptera+berlesiana+Paoli%2C+1907+%28Diptera%3A+Cecidomyiidae&accepted=accepted&btn_Search=Search.
16. Civantos, M. & Sanchez, M. Integrated control in Spanish olive groves and its influence on quality. *Agricultura Revista Agropecuaria* **62**(73), 854–858 (1993).
17. Iannotta, N., Belfiore, T., Noce, M., *et al.* & 2008, undefined. Correlation between *Bactrocera oleae* infestation and *Camarosporium dalmaticum* infection in an olive area of Southern Italy. *actahort.org* **949**, 309–316 (2012).
18. Preu, M., Frieß, J. L., Breckling, B. & Schröder, W. Case study 1: Olive Fruit Fly (Bactrocera oleae). in *Gene Drives at Tipping Points: Precautionary Technology Assessment and Governance of New Approaches to Genetically Modify Animal and Plant Populations* (Eds. von Gleich, A. & Schröder, W.) 79–101 (Springer Open, 2020). https://doi.org/10.1007/978-3-030-38934-5_4.
19. Latinović, J., Hrnčić, S., Perović, T. & Latinović, N. *Botryosphaeria dothidea*—Causal agent of olive fruit rot—Pathogen of wounds or not?. *IOBC-WPRS Bull.* **108**, 35–38 (2014).
20. Radonjić, S., Hrnčić, S. & Perović, T. Overview of fruit flies important for fruit production on the Montenegro seacoast. *Biotechnol. Agron. Soc. Environ.* **23**, 46–56 (2019).
21. Lanza, B. *et al.* A morphological analysis of fresh and brine-cured olives attacked by *Bactrocera oleae* using light microscopy and esem-eds. *Eur. J. Histochem.* **64**, 218–224 (2020).
22. Haff, R., Jackson, E., Moscetti, R. & Massantini, R. Detection of fruit-fly infestation in olives using X-ray imaging: Algorithm development and prospects. *Am. J. Agric. Sci. Technol.* https://doi.org/10.7726/ajast.2016.1001 (2016).
23. Alba-Tercedor, J. From the sample preparation to the volume rendering images of small animals: A step by step example of a procedure to carry out the micro-CT study of the leafhopper insect *Homalodisca vitripennis* (Hemiptera: Cicadellidae). in *Bruker Micro-CT Users Meeting 2014* 260–288 (Bruker-microCT-Skyscan, 2014).
24. Stalling, D., Westerhoff, M. & Hege, H.-C. Amira: A highly interactive system for visual data analysis. *Visualization Handb.* https://doi.org/10.1016/B978-012387582-2/50040-X (2005).
25. FEI. Amira 3D Visualization and Analysis Software. Preprint at (2017).
26. Alba-Tercedor, J., Alba-Alejandre, I. & Vega, F. E. Revealing the respiratory system of the coffee berry borer (*Hypothenemus hampei*; Coleoptera: Curculionidae: Scolytinae) using micro-computed tomography. *Sci. Rep.* **9**, 1–17 (2019).
27. Alba-Tercedor, J., Sáinz-Bariáin, M. & Zamora-Muñoz, C. Changing the pupal–case architecture as a survival strategy in the caddisfly Annitella amelia Sipahiler, 1998 (Insecta, Trichoptera). *Anim. Biodivers. Conserv.* **39**, 65–75 (2016).
28. Bruker microCT. How to make color-coded 3D models for structure thickness in CTVox Method note. *Bruker-Skyscan Method Notes* **25**, 1–10 (2014).
29. Haidani, A. E. *et al.* Study of the olive fruits infestation by *Bactrocera Oleae* in the area of fez in morocco and their fertility in the laboratory. *Moroccan J. Biol.* **1**, 21–31 (2004).
30. Malheiro, R., Casal, S., Pinheiro, L., Baptista, P. & Pereira, J. A. Olive cultivar and maturation process on the oviposition preference of *Bactrocera oleae* (Rossi) (Diptera: Tephritidae). *Bull. Entomol. Res.* **109**, 43–53 (2019).
31. Iannotta, N. & Scalercio, S. Susceptibility of cultivars to biotic stresses. in *Olive Germplasm—The Olive Cultivation, Table Olive and Olive Oil Industry in Italy* (ed. Muzzalupo, I.) 81–105 (InteCh, 2012).
32. Gonçalves, F. M., Rodrigues, M. C., Pereira, J. A., Thistlewood, H. & Torres, L. M. Natural mortality of immature stages of *Bactrocera oleae* (Diptera: Tephritidae) in traditional olive groves from north-eastern Portugal. *Biocontrol Sci. Technol.* **22**, 837–854 (2012).

33. Browne, F. G. The African species of Poecilips Schaufuss. *Revue de zoologie et de botanique africaines* **87**, 679–696 (1973).
34. Alba-Alejandre, I., Alba-Tercedor, J. & Vega, F. E. Observing the devastating coffee berry borer (*Hypothenemus hampei*) inside the coffee berry using micro-computed tomography. *Sci. Rep.* **8**, 17033 (2018).
35. Tzanakakis, M. E. Seasonal development and dormancy of insects and mites feeding on olive: A review. *Netherlands J. Zool.* **52**, 87–224 (2003).

Acknowledgements

This study benefited fro the following funding Grants: TED2021-130632B MCIN/AEI/https://doi.org/10.13039/501100011033 and the 'European Union NextGenerationEU/PRTR, led by F.R. The lead author J.A.-T. would like to thank the staff at Bruker micro-CT SkyScan in Kontich (Belgium) for their effective and prompt support, constant improvements to the software, and implementation of the new options requested. Special thanks to Alexander Sasov (now at NeoScan www.neoscan.com), Xuan Liu, Stephan Boons, Phil Salmon, Kjell Laperre, and Vladimir Kharitonov.

Author contributions

Conceived the study: J.A-T., F.R.; performed the micro-CT scans, software treatment to obtain rendered images, plates of figures, and Supplementary Videos preparation: J.A.-T. Analysis, interpretation of results, and manuscript preparation: J.A.-T., F.R.

Competing interests

The authors declare no competing interests.

Additional information

Supplementary Information The online version contains supplementary material available at https://doi.org/10.1038/s41598-024-72029-3.

Correspondence and requests for materials should be addressed to J.A.-T. or F.R.